Available online at www.sciencedirect.com

ScienceDirect

Procedia CIRP 124 (2024) 598–601

www.elsevier.com/locate/procedia

13th CIRP Conference on Photonic Technologies [LANE 2024], 15-19 September 2024, Fürth, Germany

# Effect of component geometry on the dynamic thermal field generated in the laser forming of AA6061-T6 sheet

Yang Fei[a]*, Ghazal Sheikholeslami[b], Tong Zhou[c], Zheng Fang[a], Yin Tang[a], Walter Perrie[a], Geoff Dearden[a], Stuart Paul Edwardson[a]

*a Laser Group, School of Engineering, University of Liverpool, Liverpool, L69 3GH, United Kingdom*
*b School of Engineering, Canterbury Christ Church University, United Kingdom*
*c College of Science, Jiangsu University of Science and Technology, China*

* Corresponding author. *E-mail address:* sgyfei2@liverpool.ac.uk

**Abstract**

Laser forming (LF) technology is an advanced, highly customizable non-contact method for shaping metal sheets, characterized by its heightened precision and flexibility. This experimental and numerical study investigates the influence of component geometry on the dynamic temperature field arising from LF of AA6061-T6 sheet metal. Finite element models were constructed to analyse the dynamic temperature field variations in plates with different dimensions. The findings demonstrate the significant effect of sheet dimensions on the induced thermal field, that consequentially affect the deformation. In contrast to a stable heating and cooling profile observed in a 50mm-wide or greater sample, a 20mm-wide or smaller sample exhibits a temperature resurgence or reflection along the laser pathway. The deformation of the aluminium plate therefore decreases with the reduction in geometry size. The analysis of this thermal behaviour helps to explain this and further advances the understanding of the LF mechanism specific to high thermal-conductivity materials.



*Keywords:* laser forming; laser bending; fibre laser, thermol field; aluminium alloy; COMSOL; finite elements analysis

## 1. Introduction

Laser forming (LF), known for its fixtureless, non-contact, and spring back free characteristics, has earned considerable attention as a sheet metal forming technique. Compared with other traditional methods, LF relies on the non-uniform temperature field generated by a defocused laser beam to produce localized thermal stresses, thereby facilitating deformation in a component. When the thermal stress exceeds the material's yield strength, it leads to plastic deformation of the component. LF has demonstrated a significant potential cost-effectiveness and customization in metal forming and adjustment.

As LF relies on the gradient temperature field generated, factors such as laser power, scanning speed, cooling conditions, cooling time active LF mechanism, and the mechanical and thermodynamic properties of the material all influence the forming result. To enhance the reliability, accuracy, and repeatability of LF technology and increase its share in industrial applications, many researchers have conducted studies in this area. M. Geiger and F. Vollertsen[1] constructed a two-layer model for analyzing the LF process and introducing the mechanism of LF, they found that the thermal expansion coefficient is one of the most important parameters influencing this process. Maji et al.[2] used the response surface methodology to find that, when using equivalent total energy input, pulsed lasers exhibit a greater bending compared to continuous lasers. Yadav et al.[3] discovered that high cooling rates significantly enhance the partial mechanical properties of duplex stainless steel, and increase bending angles. Safari[4] compared two methods, linear and curved radiation, and found that linear scanning yields greater uniformity in the curvature


10.1016/j.procir.2024.08.182

of the bent edges. Xu et al.[5] discovered that when the temperature generated by the laser beam exceeds the brittle-ductile transition threshold of silicon crystal, plastic deformation occurs in the silicon wafer. When this temperature difference in the scanning area is significant, the bending angle increases with an increasing number of laser scanning times. Bucher et al.[6] studied the behavior of sandwich panels with metal foam cores during the LF process. Their study indicated that as long as the bonding between the panel and the foam core is sufficiently strong, LF technology can be used to shape various metal foam sandwich panels. Shi et al.[7] achieved a 39-fold increase in bending angle by applying a low-temperature pre-compressive force. From this literature survey, prior research has primarily focused on the influence of laser characteristics, material properties, and scanning methods on LF forming. However, there has been limited investigation into how geometric parameters affect the forming mechanism of LF. This study aims to explore how the geometric dimensions of high-strength aluminum alloy components affect the dynamic temperature field generated during the LF process through a series of controlled experiments and by constructing finite element analysis models. The goal is to help explain and enhance the LF mechanism specific to small size metal components forming and high thermal conductivity materials.

## 2.Materials and Method

### 2.1 Experiment

A continuous-wave (CW) fiber laser (JK500) was used for laser forming experiments, with maximum power of 500W and a wavelength of 1080 nm. This is fibre delivered to a processing head mounted on a KUKA KR16R1610 6-axis industrial robot (Figure 1). Scan tool paths were designed on Autodesk Powermill. Constant processing conditions of 250W CW laser beam, 4mm spot diameter (knife edge) and 10mm/s speed were used.

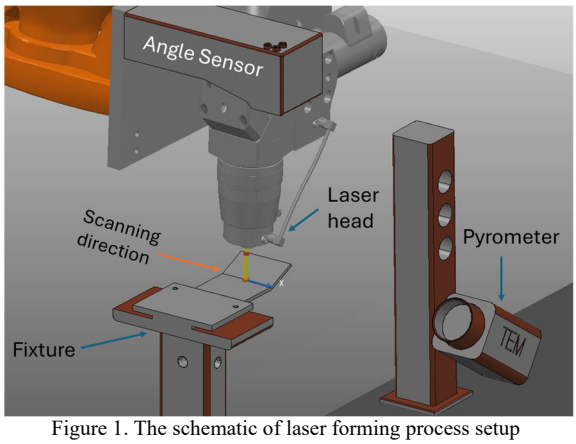


Figure 1. The schematic of laser forming process setup

The high-strength aerospace aluminium alloy AA6061-T6 was chosen as a relevant high thermal conductivity material. Aluminium alloy sheets were cut into plates of different widths, with the thickness and length kept the same. Samples were edge clamped to the fixed system bed. Scan lines were always positioned 10mm from the free end. To increase the absorption rate of the specimen to the laser, the upper surface of the specimen was covered with a thin graphite layer. The emissivity of the graphite was 0.9, measured by a thermal camera. The dimensions and sampling point locations of AA6061-T6 sheet metal are shown in Tables 1 and 2. Figure2 shows, the bottom left corner of the sample is the origin. Sampling point are used for displacement and temperature measurements both experimentally and in the FE model. To avoid interference from the graphite coating, sampling points were positioned on the reverse side of the aluminium plate and distributed along the laser scanning path at regular intervals.

Table 1. The dimensions of AA6061-T6 sheets

| Dimensions | Sheet 1 | Sheet 2 | Sheet 3 | Sheet 4 |
|---|---|---|---|---|
| Width (mm) | 20 | 30 | 40 | 50 |
| Length (mm) | 75 | 75 | 75 | 75 |
| Thickness (mm) | 1 | 1 | 1 | 1 |

Table 2. The sampling points positions of AA6061-T6 sheets (x, y, z)

| Sheets | Point1(mm) | Point2(mm) | Point3(mm) |
|---|---|---|---|
| Sheet 1 | (5,65,0) | (10,65,0) | (15,65,0) |
| Sheet 2 | (10,65,0) | (15,65,0) | (20,65,0) |
| Sheet 3 | (10,65,0) | (20,65,0) | (30,65,0) |
| Sheet 4 | (15,65,0) | (25,65,0) | (35,65,0) |

A micro epsilon laser range finder mounted to the robot is used to measure the deformation and bending angle of the samples. A micro epsilon CTM-3CF4 single point pyrometer is used for record the dynamic temperature during processing with a scan rate of 10 kHz. This has a temperature range of 250 – 1800°C.

### 2.2 Finite Element Analysis

As shown in Figure 2, The FE analysis software COMSOL6.0 was used to simulate temperature field and the stress field during the LF. In the model, room temperature is 20°C, the emissivity of AA6061-T6 is 0.3 and the natural convection coefficient between AA6061-T6 and air is 20 W/ ($m^2$.K).

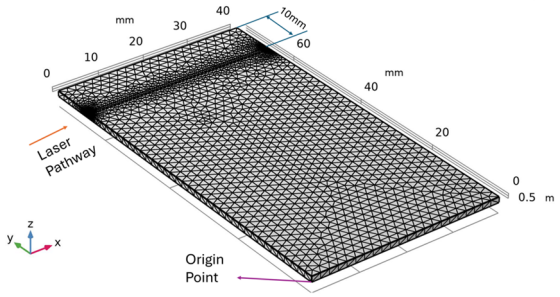


Figure 2. The mesh of the FEA model when AA6061-T6 sheet width 40mm

## 3. Results and Analysis

### 3.1 Deformation analysis

Figure 3 shows the bending angle for different sheet widths. It can be observed that when the parameters such as power, speed, and number of scans are consistent, the bending angle of the aluminium plate increases as the width of the aluminium plate increases.

### 3.2 Temperature field analysis

The temperature field generated by LF on the aluminium plate significantly influences thermal stress and the local mechanical properties of the material, playing a crucial role in the bending response. By measuring the temperature, an analysis of the differences in temperature fields for plates of various sizes was completed. Figure 4 shows the temperature curve of the middle sampling point when the sample width equals 20mm and 50mm. It can be seen in Figure 4(a) that the pyrometer only records the temperature when over 250°C. This limits the

validation of the cooling curve for the FE model, but a good agreement can be seen for the reverse surface. For a 20mm wide sample, a pronounced secondary temperature rise phenomenon was observed in both the actual temperature curve and the FE model, with the temperature and timing showing a good agreement. At 0.3248s, the FE model reached its peak temperature of 486.5°C, while the measured peak temperature was 439°C, resulting in an error of 9.77%. The first minima temperature of the FE model was 322.3°C, whereas the measured temperature was 320°C, resulting in an error of 0.713%. The second peak temperature of the FE model was 327.15°C, while the measured temperature was 323.2°C, resulting in an error of 1.21%. In contrast, when the width was 50mm, the curve during the cooling phase was smooth, gradually cooling down to room temperature. The FE model reached its peak temperature of 430.5°C at 0.3967s, while the measured peak temperature was 414.4°C, resulting in an error of 3.74%. Through comparison, it was found that the model agrees well with the actual measurement results in terms of trends and temperature. However, there are still slight differences during the cooling phase, with the model cooling faster than the actual process. This difference is mainly caused by small variations in material parameters, differences in natural convection due to varying environmental conditions, and the range and errors of the pyrometer.

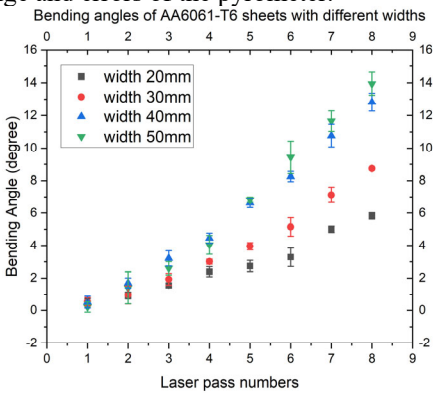


Figure. 3 The bending angle of AA6061-T6 sheets with different widths with power 250W, speed 10mm/s and spot size diameter 4mm

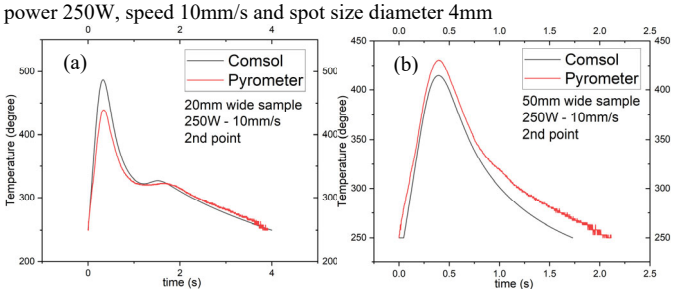


Figure. 4(a) the temperature curve of the 2nd sample point for a 20mm width. (b) the temperature curve of the 2nd sample point for a 50mm width

Figure 5 displays the temperature curves of three sampling points when the width is 40mm. The temperature re-rise only appears in the temperature curves of the third sampling points. The cooling rate at the second sampling point has significantly decreased. Closer to the plate edge, the secondary temperature rise phenomenon at the third sampling point is more pronounced. This is likely due to that as the laser beam passes through the first sampling point, the temperature of the remaining scanning area of the aluminium plate is still close to room temperature, therefore a significant amount of laser energy is consumed in heating this portion of the material. However, when the laser beam passes through the second and third sampling points, the temperature of the remaining scanning area of the AA6061-T6 plate has already risen, resulting in more heat accumulating in the scanning area with nowhere to dissipate. Natural convection in the air is insufficient to rapidly transfer this accumulated heat, leading to a rapid increase in local temperature or a slower cooling rate. Due to the closer proximity of the third sampling point to the boundary of the aluminium plate, the secondary temperature rise at this point is more significant.

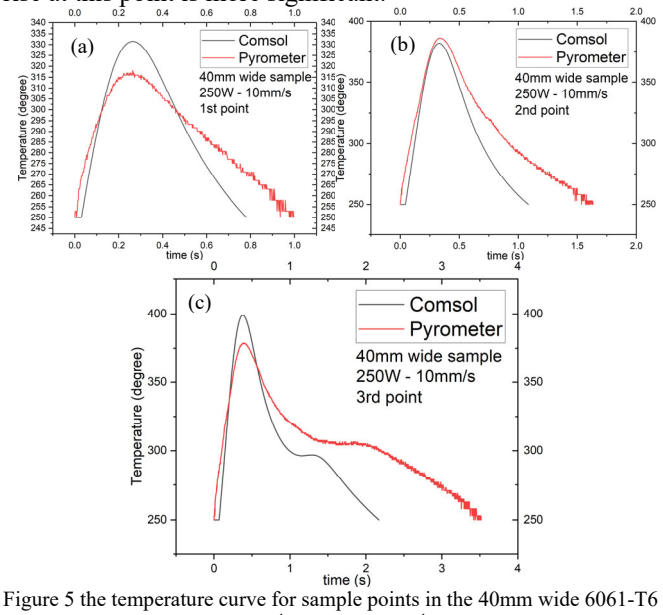


Figure 5 the temperature curve for sample points in the 40mm wide 6061-T6 sheet. (a) the 1st point. (b) the 2nd point. (c) the 3rd point

Figure 6 illustrates the dynamic evolution of the temperature field on the aluminium plate when the width is 20mm. From Figure 6(a), at the initial stage, when t=1.5s, the laser beam approaches the left boundary of the aluminium plate. The unscanned area volume is much larger than the scanned area, and the temperature of the left half of the aluminium plate is significantly higher than the right half. Heat transfer from left to right. From Figure 6(b), when t=2.5s, the laser beam just passes through the midpoint of the aluminium plate, and the temperature of the scanned area is still much higher than the unscanned area. From Figure 6(c), when t=2.8903s, the laser beam approaches the right boundary of the aluminium plate. Due to the small size of the aluminium plate, the remaining unscanned area can only absorb a small amount of heat, and a large amount of heat transfers to the left, re-heating the scanned area of the aluminium plate, causing the temperature to rise, or slowing down its cooling rate. At this time, the temperature of the second sampling point reaches the first minima, 265°. From Figure 6(d), when t=3.1833s, the laser beam leaves the surface of the aluminium plate. A large amount of remaining heat continues to diffuse to the left, continuously heating the scanned area. Currently, the temperature of the second sampling point reaches the second peak, 312°. After this, as the laser beam disappears, the aluminium plate gradually cools down to room temperature. As a comparison, Figure 7 shows the temperature curves of more sampling points when the width is 20mm. In addition of Figure 4(a), the phenomenon of this secondary temperature rise can be observed in the temperature

curves of all three sampling points. Furthermore, the peak temperature of the secondary temperature rise exhibits a gradually increasing trend. This could be due to the increasing scanning time of the laser beam, where the total energy transferred to the aluminium plate becomes greater.

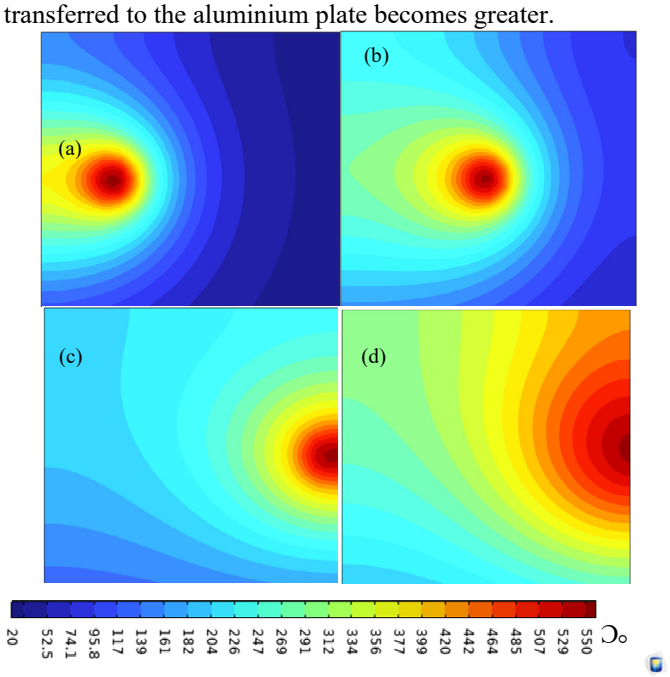


Figure. 6 the temperature field for a 20mm wide sample. (a) t=1.5s, (b) t=2s, (c) t=2.8903s, (d) t=3.1833s

Combining Figures 4(a), 5, 6 and 7, it is evident that component geometry can significantly affect the cooling phase of the dynamic temperature field, consequently altering the deformation of the aluminium alloy sheets. Particularly, when the plate width is below 20mm, the secondary temperature rise is observed across the entire scanning region. This phenomenon precipitates a significantly increase in the overall temperature of the plate, thereby reducing the temperature gradient between the upper and lower surfaces of the scanning region. Consequently, this thermal behaviour serves to suppress the bending deformation of the aluminium sheet in this experiment.

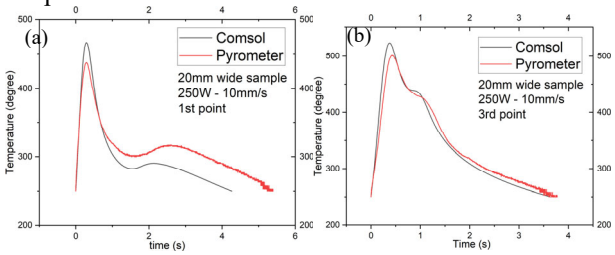


Figure.7 the temperature curve of sample points in 20mm wide AA6061-t6 sheet. (a) 1st point. (b) 3rd point

As the width of the aluminium plate increases, this unique temperature re rise effect gradually diminishes. Consequently, the effect of suppressing bending also decreases gradually with the increase in sheet width.

## Conclusion

This study focuses on the influence of component geometry on the dynamic temperature field during the LF process through experimental and numerical simulation approaches. A validated finite element model was constructed for analysing and predicting the outcomes of the LF of aluminium sheets of different widths. The following conclusions were drawn:

1. Under the same laser parameters, the application of LF technology on small-sized high thermal-conductivity aluminium alloy is more challenging.
2. When the width of the aluminium plate is small, the phenomenon of a secondary temperature rise can be observed almost throughout the entire scanning path. The overall heating rate of the scanning region is faster, and the rate of reduction in temperature difference between the upper and lower surfaces is higher, resulting in a decrease in bending angle.
3. For large-sized aluminium sheets, this thermal effect is more pronounced at the end of the laser scanning region. In other regions, it manifests as a deceleration in cooling rate.
4. For the small-sized aluminium sheets, Variable speed scanning and the addition of external forced cooling as support actions can mitigate this effect, thereby improving the forming results and accelerating the forming speed.

The clear asymmetry in the temperature field generated by forming with a single laser spot, enhanced by part geometry as shown in this work, demonstrates the need to optimise beam delivery to move the process forward. Understanding the laser forming mechanism of small metal sheets is of significant scientific importance. Such research holds the promise of significantly enhancing the potential of laser forming methods in manufacturing complex three-dimensional structures, especially in reducing spring-back in small-sized precision metal components and prototype manufacturing. The next step of the research will explore how this thermal effect influences stress and strain variations during deformation. It will study whether these changes have an effect on the microstructure and thus affect the mechanical properties of the material.

## Acknowledgment

We would like to thank Mr. Andy Snaylam (University of Liverpool) for preparing the AA6061-T6 sheets. We also thank Yin Tang, Zheng Fang, and Shuai Wang (University of Liverpool) for their help in the experimental setup.

## References

1. Geiger, M. and F. Vollertsen, *The Mechanisms of Laser Forming.* CIRP Annals, 1993. 42(1): p. 301-304.
2. Maji, K., D.K. Pratihar, and A.K. Nath, *Experimental investigations and statistical analysis of pulsed laser bending of AISI 304 stainless steel sheet.* Optics & Laser Technology, 2013. 49: p. 18-27.
3. Yadav, R., G. Vinay, and R. Kant, *Mechanical, metallurgical and corrosion analysis of forced cooling assisted laser bending of duplex-2205.* Optics & Laser Technology, 2024. 175: p. 110804.
4. Safari, M., *A comparative study on laser bending process with linear and curved irradiating schemes.* Optik, 2022. 264: p. 169426.
5. Xu, W., L.C. Zhang, and X. Wang, *Laser Bending of Silicon Sheet: Absorption Factor and Mechanisms.* Journal of Manufacturing Science and Engineering, 2013. 135(6).
6. Bucher, T., et al., *Laser Forming of Metal Foam Sandwich Panels: Effect of Panel Manufacturing Method.* Journal of Manufacturing Science and Engineering, 2019. 141(5).
7. Shi, Y., et al., *Laser bending angle and surface quality with preload at low heating temperature.* Optics & Laser Technology, 2021. 136: p. 106755.